

Artificial Neural Networks To Distinguish Charcoal from *Eucalyptus* and Native Forests Based on Their Mineral Components

Fernanda Maria Guedes Ramalho,* Geila Santos Carvalho, Paulo Ricardo Gerardi Hein, Alfredo Napoli, Robert Wojcieszak, and Luiz Roberto Guimarães Guilherme



Cite This: <https://dx.doi.org/10.1021/acs.energyfuels.0c01034>



Read Online

ACCESS |



Metrics & More



Article Recommendations

ABSTRACT: Charcoal is produced through the pyrolysis of wood. It is used as the main domestic energy source in many tropical countries from Africa and Asia, and it is used as a reductor product in the steel industry in Brazil. However, the indiscriminant use of wood from native forests is detrimental to sustainability. The development of rapid and efficient methodologies for distinguishing charcoal produced from native forest or *Eucalyptus* plantations, as found partially in Brazil, is essential to curb illegal charcoal transport and trade. The aim of this study was to distinguish charcoals from native or *Eucalyptus* woods by using artificial neural networks (ANNs) based on their mineral composition. Specimens from Brazilian native woods (*Apuleia* sp., *Cedrela* sp., *Aspidosperma* sp., *Jacaranda* sp., *Peltogyne* sp., *Dipteryx* sp., and *Gochnatia* sp.) and from *Eucalyptus* sp. hybrid woods of commercial forest plantations were pyrolyzed at temperatures from 300 °C to 700 °C in order to simulate the actual pyrolysis conditions and species widely used illegally in southeastern Brazil. Charcoals composition and proportion of mineral elements were determined by X-ray fluorescence. The ANNs were trained based on the elemental composition of the charcoal specimens to classify the species and origin of the charcoals (i.e., native forest or *Eucalyptus*). The ANNs based on mineral element content yielded high percentage of correct classification for charcoal specimens by species (72% accuracy) or origin (97% accuracy) from an independent validation sample set.

1. INTRODUCTION

Charcoal is a major source of energy in many countries. According to FAOSTAT,¹ Brazil occupies the first position among the main world producers of this product, and its consumption is concentrated in the steel industry. Extensive areas of *Eucalyptus* are cultivated to meet the demand of the steel industry in Brazil.² However, wood from native forests has been used illegally.

According to Stange et al.,³ charcoal producers have used native species from deforestation regions in tropical forests worldwide. The use of native wood for charcoal production is prohibited in many regions, because it increases the deforestation rate in the country. According to Brasil,⁴ the Brazilian government has made a national commitment to reduce 40% of the annual rates of deforestation in the Cerrado biome. In 2016, charcoal manufacture from native forests reduced 31.7%.⁵ However, enforcement actions to stop the production, transport, and trade of illegally produced charcoal are insufficient, because there is no official information about illegal operations. Under these circumstances, although a conservation priority hotspot, the Brazilian Cerrado is one of the most threatened biomes in the country.⁶

Fraud is difficult to identify, because of the similarity between charcoals when observed with the naked eye.⁷ Also, identification of charcoal by anatomical analysis is time-consuming and requires highly trained technicians.⁶ Alternative techniques for charcoal classification have been investigated, such as image analysis,^{8,9} where some wood characteristics are

extracted and analyzed to discriminate among the precursory species. Moreover, several studies have shown promising results, applying spectrum-based processing systems for classifying charcoal,^{10,7,11} but many limitations must be overcome to apply these models in real situations where pyrolysis temperature and species are unknown and must be used within the models.

The possibility of differentiating charcoals produced from planted or native wood based on the mineral composition of charcoal was examined in the present study via X-ray fluorescence (XRF), which is a technique used in analytical routines to identify and measure mineral elements in solid or liquid samples.¹² This technique is versatile and does not require exhaustive preparation of the material to be analyzed.¹³ Because of that, XRF spectroscopy has been successfully applied in various fields of science that require rapid analytical routines such as agriculture,¹⁴ soil science,¹⁵ mining,¹⁶ and environmental sciences,¹⁷ as well as chemical¹⁸ and archeological studies.¹⁹

Faced with the challenge of differentiating charcoal produced from planted or native wood, the hypothesis of

Received: April 1, 2020

Revised: June 13, 2020



Table 1. Pyrolysis Plan As a Function of Biological Material, Temperature, and Number of Samples

vegetal material	code	Furnace		Number of Specimens by Temperature				
		ATG	muffle	300 °C	400 °C	500 °C	600 °C	700 °C
<i>Apuleia</i> sp.	A	×		5		6		6
<i>Cedrela</i> sp.	C	×		4		6		6
<i>Aspidosperma</i> sp.	P	×		5		6		6
<i>Jacaranda</i> sp.	J	×		5		6		6
<i>Eucalyptus</i> sp. (1) ^a	Ec	×		5		6		6
<i>Eucalyptus</i> sp. (2) ^b	Ev	×		5		6		6
<i>Peltogyne</i> sp.	R		×		2	2	2	2
<i>Dipteryx</i> sp.	U		×		2	2	2	2
<i>Gochnatia</i> sp.	B		×		2	2	2	2
<i>Eucalyptus</i> sp. (1) ^a	Ec		×		2	2	2	2
<i>Eucalyptus</i> sp. (2) ^b	Ev		×		2	2	2	2

^a*Eucalyptus* sp. (1): reforestation hybrids managed for charcoal production. ^b*Eucalyptus* sp. (2): reforestation hybrids managed for pulp and paper industry.

this study is that the mineral composition of charcoal varies according to whether trees have grown in native or planted forest. While native plants rely on the natural composition of their environment to grow, soils of forest plantations are managed for production of wood for pulp or bioenergy industries in such a way that mineral contents are adjusted before planting, which affects the mineral composition of the plant. Some studies support our hypothesis, although they were not designed to evaluate this issue.^{20,21} In fact, Kim et al.²⁰ have evaluated inorganic metals in oak, *Eucalyptus*, Pinus, and Japanese cedar biochars by means of XRF spectrometry. They reported the presence of Si, K, Ca, Al, Mg, Na, P, and Fe in all studied materials, but in different concentrations: oak, pitch pine, and Japanese cedar present much more Si, Ca, K, Al, and Na than *Eucalyptus* charcoals. The above results clearly show that *Eucalyptus* wood has a very different ash composition from other biomasses. But, again, Kim et al.²⁰ and Brewer et al.²¹ did not design their studies to evaluate the potential of XRF spectrometry to detect the origin of biochars precursor raw material.

In this study, artificial neural networks (ANNs) were developed to evaluate the complex information on the mineral composition of charcoal specimens. ANNs are computational techniques based on mathematical models capable of classifying and predicting material properties.²² The ANN approach has been successfully applied in different fields of forest sciences, such as wood defect detection,²³ wood veneer classification,²⁴ and wood species classification.^{25,26} ANNs have also shown efficiency in assessing several biochar properties. Yang et al.²⁷ evaluated the adsorption potential of bamboo biochar for dyes of metal complexes using ANNs. Moreover, Selvanathan et al.²⁸ used modeling by feedforward back-propagation (FFBP) neural networks to predict the weight loss of biomass in the pyrolysis process and copper concentration for adsorption reactions using biochar derived from rambutan shell (*Nephelium lappaceum*). Liao et al.²⁹ developed multilayer feedforward ANNs to predict the total yield and surface area of activated carbon produced from various biomass raw materials using pyrolysis and steam activation. Also, Cao et al.³⁰ studied an intelligent modeling approach using ANNs to predict the biochar yield of cattle manure pyrolysis.

Most studies that have applied ANNs to wood and its coproducts have reported promising results for classification or estimation of properties. However, to our knowledge, there is

no study involving ANNs for charcoal classification by origin, or for identification of the precursor wood species. Thus, the aim of this study was to develop ANNs to classify the origin of charcoal (i.e., native or planted forest) and the precursor species based on their mineral composition.

2. MATERIALS AND METHODS

2.1. Materials. Native tropical wood species from the Cerrado and Amazon biomes and reforestation were used in this study. The native species were *Cedrela* sp. (Cedar, labeled as “C”), *Aspidosperma* sp. (Peroba, labeled as “P”), *Jacaranda* sp. (Rosewood, labeled as “J”), *Apuleia* sp. (Garapa labeled as “A”), *Peltogyne* sp. (Pau-roxo, labeled as “R”), *Dipteryx* sp. (Cumaru, labeled as “U”), and *Gochnatia* sp. (Cambará, labeled as “B”).

As for reforestation, two genetic materials from two forest companies were used as representative hybrids of the sector. One company produces charcoal (6.5 years old *Eucalyptus grandis* × *E. urophylla* hybrid clones labeled “Ev”) and the other one produces paper and pulp (6 years old *Eucalyptus grandis* × *E. urophylla* hybrid clones labeled “Ec”).⁷ The seven native species occur in the two largest Brazilian biomes, while *Eucalyptus* hybrids were selected to represent the genetic variation that exists between the clonal materials used in reforestation by forestry companies in the country. Table 1 lists the species, furnaces, and temperatures used to generate the dataset of this study.

2.2. Specimen Preparation. Central boards were removed from trees. A total of 141 specimens (defect-free) were obtained from native and *Eucalyptus* trees. From the native species, 91 specimens presenting the dimensions of 3.5 cm × 3.5 cm × 4.5 cm (R × T × L) and 3.5 cm × 3.5 cm × 10 cm were produced while 50 specimens (defect free) of *Eucalyptus* were produced with dimensions of 2.5 cm × 2.5 cm × 10 cm (R × T × L). Sampling was properly identified using a special pencil (labeling did not disappear after pyrolysis). Before pyrolysis, the wood specimens were kept in an acclimatized room until reaching 12% moisture.

2.3. Pyrolysis Process. Wood specimens were pyrolyzed in two laboratory ovens: a Macro ATG oven and a muffle furnace, respectively developed by the Center of International Cooperation in Agronomic Research for Development (CIRAD, France) and by Universidade Federal de Lavras (UFLA, Brazil).

2.3.1. Macro ATG Furnace. The Macro ATG prototype is equipped with an oven that can reach 1000 °C, a pyrolysis reactor pressure controller, a condensable gas condenser, a load cell, a gas chromatography flow meter, a control panel, and software. Experiments can be developed using various gases simulating various conditions of partial or complete combustion in the presence of an inert atmosphere.^{31,7}

Wood specimens were added in a crucible for pyrolysis in the Macro ATG. The temperature inside the system was monitored by

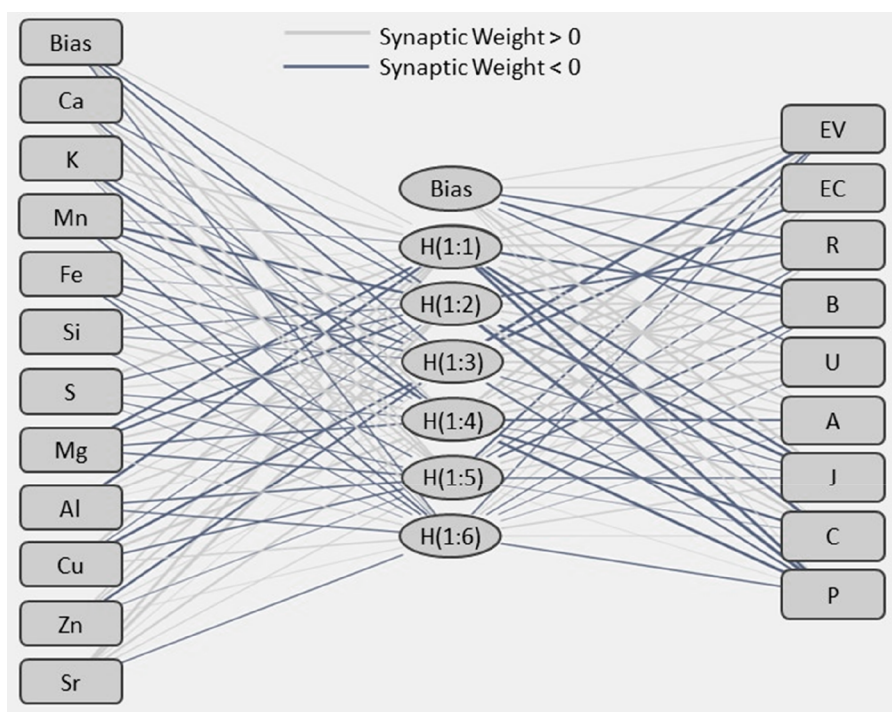


Figure 1. Network diagram to estimate the wood species of charcoal based on the mineral composition.

means of four thermocouples, and the gases resulting from the pyrolysis process were condensed by means of a condenser attached to the oven. After the prototype cooling period, the charcoals were removed and brought to moisture stabilization in a climate room. The pyrolysis of the specimens was conducted at an initial temperature of 40 °C, a heating rate of 5 °C min⁻¹ and remained for 1 h at the final temperatures of 300, 500, and 700 °C. After the process of converting wood to charcoal, the material remained inside the oven for cooling for 15 h.⁷

The biological materials carbonized in the Macro ATG oven were *Apuleia* sp., *Cedrela* sp., *Aspidosperma* sp. (Peroba), *Jacaranda* sp. (Jacarandá), and *Eucalyptus*, resulting in 101 specimens divided into three pyrolysis temperatures.

2.3.2. Muffle Furnace. Operating conditions for specimens pyrolyzed in a muffle furnace (electric; model Q318M; Quimis, São Paulo, Brazil) were as follows: initial temperature, 100 °C; heating rate, 100 °C h⁻¹; 30 min at final temperatures of 400, 500, 600, and 700 °C and 16 h after completion of the conversion process.

The wood specimens were carbonized within a pyrolysis capsule placed inside the muffle furnace. The pyrolysis capsule was connected to a water-cooled condenser coupled to a receiver flask of condensable gases. The charcoal specimens were produced at 400, 500, 600, and 700 °C to simulate the temperature range adopted in real situations in most Brazilian industries.

The biological materials carbonized in the muffle furnace were *Peltogyne* sp., *Dipteryx* sp., *Gochnatia* sp., and, again, *Eucalyptus*, resulting in 40 specimens, divided into four pyrolysis temperatures.

The different furnaces and temperatures were used to verify the influence of the conversion process on material distinction and to simulate the thermal variation that occurs in an industrial and conventional furnace. After the furnaces were cooled, the charcoals produced were removed and taken to a climate room until moisture stabilization occurred.

2.4. X-ray Fluorescence Spectrometer. In order to simulate a variation source, the determination of mineral elements was performed using two XRF spectrometers: a M4 Tornado and a S8 Tiger spectrometer.

2.4.1. M4 Tornado. An energy-dispersive X Ray fluorescence (EDXRF) spectrometer (Model M4 Tornado, Bruker Nano GmbH,

Berlin, Germany) was used to determine and quantify the mineral elements present in the different charcoal samples.

The X-ray tube of this commercial benchtop spectrometer is a microfocus side window Rh tube powered by a low-power HV generator and cooled by air. A polycapillary lens is used to obtain a spot size down to 25 μm for Mo Kα radiation. The X-ray generator was operated at 50 kV and 600 μA and a composition of filters was used to reduce background (100 μm Al/50 μm Ti/25 μm Cu). Detection of the fluorescence radiation is conducted using a thermoelectrically cooled silicon-drift-detector with energy resolution of 142 eV for 5.9 keV (Mn Kα). Measurements were performed under 20 mbar vacuum conditions to avoid back diffusion and improve detection limits.

A built-in camera allows one to visualize the studied area and the analysis was fully automated and unattended. The counting time and the scanning spatial resolution is freely selected, according to the required resolution. The sample was mounted directly on a Table 360 mm × 260 mm, which was attached to a stage translatable along the XY axis. The scanning step size used was 25 μm, and the time per analyzed point was 0.5 ms × 3 cycles. Each selected area was analyzed over a period to accumulate sufficient data points for high-resolution mapping. Data output was obtained through the X-ray intensity of specific X-ray peaks corresponding to the element signals measured in each point defined by its X and Y coordinate (μm). The data were converted using the software into a data matrix, from which XY contour maps (two-dimensional (2D) maps) of the data were generated for each element.³²

The analysis was performed on five specimens of each charcoal produced at different temperatures in the Macro ATG furnace. Each charcoal specimen was placed inside the equipment and a rectangular area was selected for irradiation during the analysis. In this area, 100 points were analyzed and the resulting spectrum was the average of all these points.

Treatment of the X-ray spectra, analyses of the peaks, and determination of which mineral elements are present in each sample and in what quantity were conducted using the M4 Tornado software.

2.4.2. S8 Tiger. A wavelength-dispersive X-ray fluorescence (WDXRF) spectrometer (Model S8 Tiger, Kennewick, WA, USA) was also used to determine and quantify the mineral elements present in the different charcoal samples.

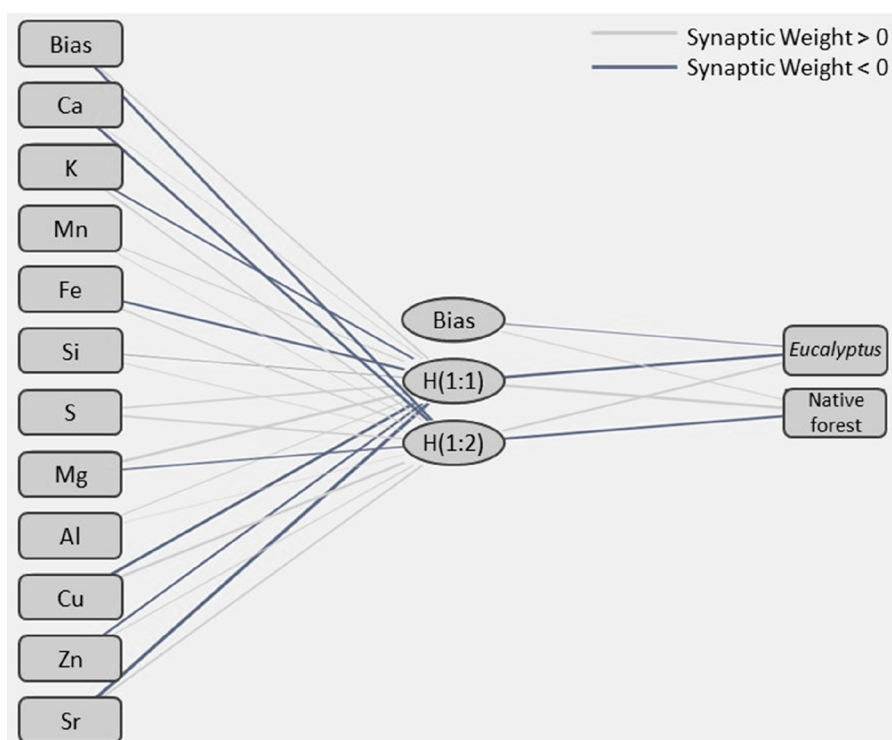


Figure 2. Network diagram to estimate the wooden origin (native forest or Eucalypt plantation) of charcoal based on the mineral composition.

Using the 150- μm fraction of different charcoal samples, pressed flat dies (3.4 cm of diameter) were obtained using an automatic press machine (Vaneox model – Fluxana) applying 25 ton cm^{-2} . Each pellet was obtained by mixing 4.5 g of ground charcoal and 3.5 g of Hoechst wax C micropowder (Merck- $\text{C}_{38}\text{H}_{76}\text{N}_2\text{O}_2$). The pellets were screened using a WDXRF spectrometer (Model S8 Tiger 4 kW, Bruker). The analysis was performed by scanning the full length of the sample surface.

This spectrometer was equipped with a Rh X-ray tube (60 kV maximum) with 75 μm Be window; analyzer crystals - (LiF200, LiF220, PET, XS-55 and XS-C): 20–60 kV, 5–170 mA, 4 kW excitation power; two detectors (flow and scintillation counter); two filters (Al and Cu), two collimators (0.23 and 0.46°); and one beam mask (34 mm). The box for automatic loading has a 60-sample capability. The analyses were conducted using the Bruker Quant-Express and GeoQuant methods. For this standardless method, after an internal calibration check, the following results (mg kg^{-1}) were found (certified/obtained): Na_2O (13.94/13.82), Al_2O_3 159 (1.22/1.21), SiO_2 (71.08/71.21), SO_3 (0.57/0.56), Cl (0.25/0.26), K_2O (5.01/5.01), CaO 160 (5.13/5.16), Fe_2O_3 (0.07/0.08), SrO (1.97/1.94), and Sb_2O_3 (0.66/0.65). For data spectral acquisition, processing, identification, and quantification of the elements, the software Spectraplus 2.2.3.2 (Geo-quant test) was used. Measurements were made under a vacuum system.

2.5. Artificial Neural Network. ANNs were developed using a feedforward multilayer perceptron (MLP) algorithm. The mineral contents of charcoal specimens were used as input variables, while the wood species or charcoal origin comprised the output variables. The ANNs of the present study were developed using the SPSS statistical software (v. 20).

2.5.1. Network Architectures. The optimal network architectures were established by trying different combinations of number of hidden layers (1 or 2) and neurons (1–9). ANN 1 has six neurons in the hidden layer and nine output layer neurons, which represent the nine wood species converted to charcoal specimens (*Eucalyptus*, *Peltogyne* sp., *Gochnatia* sp., *Dipteryx* sp., *Apuleia* sp., *Jacaranda* sp., *Aspidosperma* sp., and *Cedrela* sp.), while ANN 2 presented two (2) hidden layer neurons and two (2) output layer neurons, which represent the origin of the charcoal (native forest or *Eucalyptus*). The

maximum number of epochs of each ANN was 100. The diagrams of the ANNs designed for species and for origin are shown in Figures 1 and 2, respectively.

Every neuron is in a hidden layer and the output layer represents an activation function. In this study, a hyperbolic tangent sigmoid function was used as the activation function in the hidden layers, while the output layer activation function was softmax. General information on the ANN for classifying wood species or charcoal origin based on mineral composition is listed in Table 2.

2.5.2. Covariate Sets for ANN. The model inputs (covariables) were the concentration values of the mineral components present in the charcoal and the output of the model were species (ANN1) or origin (ANN2). For ANNs, 11 (11) explanatory variables (Ca, K, Mn, Fe, Si, S, Mg, Al, Cu, Zn, and Sr, hereafter called covariates) were considered for training the ANN to classify the species (ANN1) or origin (ANN2) of charcoals (see Table 2). Data were normalized before developing ANNs.

2.5.3. Network Training and Validations. ANN models were validated by test sets. To guarantee homogeneity between training and validation sets, the selection of the samples of each subset was done manually. The sample set (142 observations) was ranked by species, temperature, and origin and the dataset was split into two uniformly distributed subsets. This procedure allowed higher control of the variability within each subset: the calibration set was composed of 95 specimens, while the test set had 47 samples with mineral composition information. The selection of ANN models was based on the percentage of correct classifications, with regard to the different species of charcoal (ANN1) or their origin (ANN2).

3. RESULTS AND DISCUSSION

3.1. Mineral Composition Variation of Charcoal. The mineral elements present in the charcoals produced from different species and under different pyrolysis temperatures were detected by XRF analysis. Table 3 presents the mean values as a percentage of the elemental composition of the native and planted wood charcoal samples.

Table 2. Information from Artificial Neural Networks To Classify the Origin of Charcoals Based on Their Mineral Components

variable	Information	
	ANN 1	ANN 2
Input Layers		
Covariate 1	Ca	Ca
Covariate 2	K	K
Covariate 3	Mn	Mn
Covariate 4	Fe	Fe
Covariate 5	Si	Si
Covariate 6	S	S
Covariate 7	Mg	Mg
Covariate 8	Al	Al
Covariate 9	Cu	Cu
Covariate 10	Zn	Zn
Covariate 11	Sr	Sr
number of units	11	11
rescaling method for covariates	standardized	standardized
Hidden Layer		
number of hidden layers, <i>N</i>	1	1
number of units in the first hidden layer	6	2
activation function	hyperbolic tangent	hyperbolic tangent
Output Layer		
dependent variables	wood species	native or Eucalyptus
number of units, <i>N</i>	9	2
activation function	softmax	softmax
error function	cross-entropy	cross-entropy

The results show that minerals such as calcium (Ca) and iron (Fe) present higher proportion, relative to the others. In addition to varying by species, the percentage of minerals also varies as the pyrolysis temperature increases, yet no trend was detected. These variations are important for training the artificial networks to classify the charcoal by its origin. Although the data does not have a clear tendency detectable by visual analysis, the ANN can recognize nonlinear data patterns.

There are few studies that have evaluated the composition and proportion of mineral elements in charcoal or forest biomass. Kim et al.²⁰ have evaluated inorganic metals in oak, *Eucalyptus*, pine, and Japanese cedar biochars via XRF spectrometry and found Si, K, Ca, Al, Mg, Na, P, and Fe in all studied materials. The elements that stood out in *Eucalyptus* were Si, K, and Ca. In the present study, the last two elements are present in high percentage. Brewer et al.²¹ studied the ash composition of Switchgrass (grass), maize straw, and hardwood (unspecified) samples via XRF spectroscopy using the pressed tablet method and found Al₂O₃, CaO, Cl, Fe₂O₃, K₂O, MgO, MnO₂, Na₂O, P₂O₅, SiO₂, and SO₃ in all varieties studied, with CaO presenting the highest percentage (22.37%) for wood. Bouraoui et al.³³ have analyzed the mineral content of faveira and found significant amounts of silicon (4430 mg kg⁻¹), calcium (1260 mg kg⁻¹), and potassium (990 mg kg⁻¹), while magnesium was detected in smaller amounts (550 mg kg⁻¹). All minerals reported by Bouraoui et al.³³ were found in the charcoal samples analyzed in the present study.

3.2. Neural Network Architecture. The ANN architectures developed in this study are presented, respectively, in Figures 1 and 2, along with their respective input layers, hidden

layers, neurons, output layers, and synaptic weights. Both ANNs used to estimate charcoal origination as a function of wooden species (Figure 1) as well as origin (i.e., native forest or *Eucalyptus* plantation) (Figure 2) were obtained using 11 input neurons and 1 hidden layer, with 6 and 2 neurons respectively.

Synaptic weights represent the connecting forces between neurons and are used to store acquired knowledge.³⁴ Weight is considered excitatory when it is positive (>0) and inhibitory when it is negative (<0). High synaptic weights are indicated by thick lines while low weights are represented by thin connections. A synaptic weight greater than zero is indicated in light gray, while a synaptic weight below zero is indicated in dark gray (Figures 1 and 2). Since very negative or very positive weights can generate thicker connections, the more positive or the more negative a weight, the thicker the connection. Input variables can be evaluated by considering the connections between the hidden layer or the output layer.

The two ANN models were developed based on the values of the proportion of mineral components present in the material to estimate the origination of the charcoals, as a function of wood species and as a function of origin classes, i.e., native forest or *Eucalyptus* plantation. For ANN 1 (Figure 1) the thick connections with very negative synaptic weights occurred at the Ca, K, Si, S, Mg, Al, Cu, Zn, and Sr inputs and those with very positive weights occurred at the Ca, K, Mn, Fe, S, Mg, Al, Cu, and Zn inputs (see Table 4). For ANN 2 (Figure 2), the very negative weights were highlighted in the K, Fe, Si, Cu, Zn, and Sr inputs and very positive ones occurred in the Ca, Mn, S, Mg and Al inputs (Table 5). Since the quality of data can affect the performance of the ANN, it is very important to observe whether the data are adequate. The thicker, very positive and negative connections indicate that the input variable is important to define the output variable. In fact, most of the mineral elements used in the input layer had such connections.

3.3. Identification of the Charcoal Origin. The model for classifying species (ANN 1, Table 6) was able to correctly predict 88.3% of the specimens of the independent test set and 74.5% of specimens belonging to the training set. Of the erroneous classifications in the test set, only two specimens of the native genus (*Jacaranda*) were confused with *Eucalyptus* specimens and only one specimen from plantation (*Eucalyptus*) was classified as *Peroba* (native). Most incorrect predictions were of the genera of native specimens among themselves or *Eucalyptus* specimens among themselves. This type of error within each category is positive for classification purposes, because it is possible to identify illegal native charcoals, regardless of the tree genus.

The model to classify the origin (native or *Eucalyptus*) of charcoal (ANN 2, Table 7) was able to estimate the classes correctly with 97.9% success in the test set. Only one native specimen was misclassified as *Eucalyptus*, and the entire remaining set was correctly predicted. This finding indicates that the use of ANNs can be an efficient tool for classifying charcoal samples, based on the proportion of mineral elements as input data. In addition to the high percentage of correct classifications, the only error that occurred should not lead to an accusation of false fraud, which would be serious if the error is to classify *Eucalyptus* charcoal (legal) as native charcoal (mostly illegal).

ANNs have proven to be a powerful machine learning tool for function approximation and pattern recognition. ANN has

Table 3. Averaged Mineral Composition of Charcoal by Wooden Species and Pyrolysis Temperature

species ^a	temperature (°C)	Percentage (%)										
		Ca	K	Mn	Fe	Si	S	Mg	Al	Cu	Zn	Sr
EV	300	21.08	3.59	2.77	42.07	3.16	0.28	1.92	4.12	1.21	2.60	1.27
	400	65.96	13.84	5.00	3.06	3.32	1.65	1.17	1.46	0.97	1.27	2.91
	500	31.33	13.58	4.64	36.39	1.95	0.69	0.76	1.30	1.29	1.19	1.32
	600	23.06	2.87	3.29	2.69	17.21	1.56	1.39	5.94	0.88	0.93	3.10
	700	27.37	19.41	3.26	23.75	9.85	1.37	0.52	4.55	1.18	1.52	1.28
EC	300	19.37	5.27	2.36	42.40	4.39	0.11	1.79	6.75	1.23	3.03	1.52
	400	53.81	24.36	2.72	2.15	3.59	2.29	2.09	1.32	1.20	1.46	3.10
	500	30.34	22.92	1.78	22.83	2.61	0.64	0.71	1.31	0.64	0.77	1.30
	600	22.78	32.93	1.49	2.32	5.68	1.51	1.05	3.76	1.00	1.00	2.54
	700	38.06	17.31	1.80	25.14	4.29	0.97	0.47	2.41	0.91	1.22	1.51
R	400	74.42	6.36	3.04	0.83	2.08	1.66	5.37	0.49	1.15	0.68	3.99
	500	78.75	4.55	2.89	0.57	0.89	1.47	5.23	0.32	0.87	0.49	4.34
	600	74.54	5.04	5.07	0.59	1.14	1.38	6.83	0.14	1.52	0.52	4.37
	700	79.34	4.24	3.24	0.46	0.74	1.32	5.38	0.99	0.99	0.28	4.41
B	400	4.59	4.38	0.57	0.50	12.07	1.49	0.51	75.09	0.30	0.45	0.57
	500	4.96	1.16	0.28	0.54	14.85	0.97	0.73	74.62	0.39	0.44	0.50
	600	5.46	1.64	0.31	0.68	12.42	0.94	1.07	66.31	0.41	0.38	0.66
	700	5.56	2.47	0.35	0.61	21.92	1.27	1.62	64.76	0.39	0.43	0.55
U	400	81.66	1.38	2.33	0.83	6.38	0.66	0.80	2.24	0.40	0.18	2.91
	500	76.72	2.56	1.68	1.18	9.08	0.88	0.93	3.22	0.65	0.36	2.31
	600	64.70	3.26	2.91	1.72	15.63	0.87	1.17	5.83	0.63	0.32	2.51
	700	67.89	2.57	2.53	1.40	14.66	0.70	0.98	5.35	0.39	0.23	2.60
A	300	53.60	13.90	1.62	6.22	0.22	1.56	1.73	0.90	0.34	0.87	1.08
	500	57.98	21.54	1.27	9.53	0.15	1.47	1.51	0.52	0.40	0.84	0.81
	700	62.96	23.28	1.31	6.26	0.17	0.85	0.91	0.43	0.28	0.58	0.77
J	300	48.09	1.31	2.53	21.00	1.98	0.35	4.24	3.09	0.63	0.65	1.24
	500	66.62	5.42	3.91	11.98	0.50	0.53	2.25	0.45	1.09	0.93	0.98
	700	62.91	1.14	3.38	14.80	1.26	1.01	3.91	1.20	0.96	0.96	0.68
C	300	57.98	6.16	0.21	5.27	1.08	0.17	3.60	2.11	0.33	1.01	1.87
	500	61.42	10.18	0.34	14.45	1.25	0.78	2.30	0.99	0.32	0.79	1.18
	700	69.02	8.87	0.49	10.56	0.33	0.35	2.66	0.58	0.34	0.86	1.38
P	300	46.07	21.81	7.89	1.38	3.16	0.19	1.79	11.30	0.17	1.25	1.50
	500	38.31	27.11	7.37	11.71	1.22	0.21	1.99	6.48	0.13	0.73	1.04
	700	47.95	13.31	6.48	8.13	2.13	0.31	4.16	11.98	0.28	0.66	1.08

^aAbbreviations: EV, *Eucalyptus*; EC, *Eucalyptus*; R, *Peltogyne* sp.; B, *Gochnatia* sp.; U, *Dipteryx* sp.; A, *Apuleia* sp.; J, *Jacaranda* sp.; P, *Aspidosperma* sp.; and C, *Cedrela* sp.

been applied as a modeling tool to overcome various challenges in many timber forestry sectors. Some studies have developed ANN models to estimate wood density,^{35,36} wood stiffness,³⁷ and wood strength,³⁸ as well as to assess the surface quality of wood³⁹ and to predict the moisture content of wood during drying.^{40,41} With respect to the application of the ANN approach in classifications, most studies have shown promising findings as well as ours. For instance, Cui et al.²⁶ have used laser-induced breakdown spectroscopy (LIBS) combined with ANN to classify four wood species and reported a correct specimen classification rate of 100% in the test set, using a model with a multilayer perceptron network and the Broyden–Fletcher–Goldfarb–Shanno iterative algorithm. Nisgoski et al.²⁵ have

compared ANN and SIMCA classifications to identify some Brazilian wood species based on near-infrared spectra. Their neural network resulted in no misidentification for a $\pm 2\%$ margin using a spectral range of 10 000 to 4000 cm^{-1} , while SIMCA produced over 60% misidentification, using the raw spectra. Esteban et al.⁴² have developed ANNs to differentiate wood from *Pinus sylvestris* and *Pinus nigra* and their network achieved 90.4% accuracy for the training set and 81.2% for the validation in the test set. Wenshu et al.²³ have studied the detection of defects in wood board based on ANN with an identification success rate of 86.67%. Castellani and Rowlands²⁴ have built an evolutionary ANN for classifying wood veneers from statistical characteristics of wood subimages. Experimental evidence from this study showed that their

Table 4. Training Parameters of Artificial Neural Network 1 (ANN 1) Used To Estimate the Origin of Charcoal Based on Mineral Components

Predictor		Predicted								
		Hidden Layer 1								
		H(1:1)	H(1:2)	H(1:3)	H(1:4)	H(1:5)	H(1:6)			
Input Layer	(Bias)	0.293	−0.499	−0.544	0.753	0.461	−0.284			
	Ca	0.013	−0.392	0.610	−0.438	0.786	0.471			
	K	1.485	0.215	−0.169	−1.404	0.787	−0.022			
	Mn	−0.073	−2.817	−1.104	−0.122	0.198	−0.530			
	Fe	0.064	−0.008	−0.654	−0.134	−0.345	−0.430			
	Si	0.409	−0.338	−0.271	1.225	0.053	−0.219			
	S	1.658	−0.535	0.382	−0.378	−0.364	−0.002			
	Mg	−1.414	−1.397	1.567	−0.824	−0.736	0.433			
	Al	−1.390	0.289	1.046	0.029	−0.919	−0.503			
	Cu	1.317	−0.170	−1.491	2.003	−0.665	0.501			
	Zn	0.450	0.721	−0.996	0.074	−0.109	0.091			
	Sr	1.062	1.577	0.010	0.677	0.211	−0.397			
		Output Layer								
		[Ev]	[Ec]	[R]	[B]	[U]	[A]	[J]	[C]	[P]
Hidden Layer 1	(Bias)	0.217	1.180	−1.027	−1.556	−0.467	0.102	1.570	0.111	0.082
	H(1:1)	0.877	0.564	1.804	−1.832	1.194	2.084	−1.545	−1.673	−1.519
	H(1:2)	0.287	2.227	−1.288	0.818	1.213	0.295	−1.926	1.690	−2.486
	H(1:3)	−3.054	−2.728	2.124	1.777	1.177	0.858	−0.354	0.653	−0.714
	H(1:4)	1.726	0.398	1.305	1.671	1.838	−2.785	−0.152	−1.796	−2.561
	H(1:5)	−0.622	0.534	−0.336	−0.879	1.041	0.444	−0.483	−0.061	0.009
	H(1:6)	−0.306	0.004	0.385	−0.226	−0.130	−0.007	0.659	0.185	−0.619

Table 5. Training Parameters of Artificial Neural Network (ANN 2) Used To Estimate the Origin of Charcoal Based on Mineral Components

Predictor		Predicted			
		Hidden Layer 1		Output Layer	
		H(1:1)	H(1:2)	<i>Eucalyptus</i>	native forest
Input Layer	(Bias)	0.383	−0.605		
	Ca	0.103	−0.663		
	K	−0.467	0.403		
	Mn	0.374	0.145		
	Fe	−0.882	0.429		
	Si	−0.052	0.224		
	S	0.542	0.553		
	Mg	1.559	−0.455		
	Al	0.265	0.098		
	Cu	−0.922	0.840		
	Zn	−0.486	0.258		
	Sr	−1.038	0.450		
Hidden Layer 1	(Bias)			−0.256	0.370
	H(1:1)			−1.807	1.933
	H(1:2)			0.813	−0.911

treatment temperature,^{38,44} tree age,³⁵ wood species,⁴⁴ basic density,³⁵ basal area (in m² ha^{−1}), annual average increment (in m³ ha^{−1} yr^{−1}), total height and diameter at 1.3 m from the ground.³⁵ This study is pioneering in its use of mineral elements contained in charcoals as predictive variables in ANN modeling.

3.4. Limitations of This Study. The rapid identification of charcoal origin can be performed through the ANNs developed in this exploratory study. The approach used in this study shows that it is possible to create an automated process to determine the legality of the charcoal load and then reduce the fraudulent charcoal trade. However, robust models may be further developed, taking into account more wood species and pyrolysis process conditions. Complementary studies are necessary to build robust data of charcoal mineral composition, including samples of several wood species, regions, pyrolysis kilns, temperatures, dimensions, moisture, etc. Models generated in this research can be fed with new information on mineral content of other forest species to ensure greater applicability. Thus, they can be used to identify a greater variety of forest species. The model's functionality shows that the mineral components associated with ANNs are factors that contain useful information capable of identifying unknown charcoals. This innovative approach can be used by other researchers and professionals to apply in their realities.

4. CONCLUSION

The findings reported in this study show the great potential for the use of ANNs as systems to identify the charcoal origination when traditional qualitative or quantitative methods cannot be used. This same approach can be used by other researchers and professionals to be applied in their working conditions. Models can be fed with information from other forest species to

algorithm builds highly compact multilayer perceptron structures capable of accurate and robust learning. The studies reported above show that ANNs are robust techniques capable of analyzing complex data. To our knowledge, no study has applied neural networks for charcoal classifications, especially to evaluate the mineral composition of charcoal. The data used as input variables in ANN for evaluating wood can be physical and mechanical characteristics,⁴³ heat

Table 6. ANN Classification of Charcoal by Wood Species (Ev, Ec, R, B, U, A, J, C, and P)^a Using the Mineral Composition of the Charcoals Produced at Temperatures from 300 °C to 700 °C

observed	Predicted by ANN									correct classification (%)
	EV	EC	R	B	U	A	J	C	P	
Training Set										
EV	12	5								70.6
EC	3	13						1		76.5
R			5							100.0
B				5						100.0
U					6					100.0
A						11				100.0
J							10		1	90.9
C								11		100.0
P							1		10	90.9
overall percentage (%)	16.0	19.1	5.3	5.3	6.4	11.7	11.7	12.8	11.7	88.3
Test Set										
EV	5	2							1	62.5
EC	1	7								87.5
R			3							100.0
B				3						100.0
U					2					100.0
A						2	1	2	1	33.3
J	1	1					4			66.7
C						1		3	1	60.0
P									6	100.0
overall percentage (%)	14.9	21.3	6.4	6.4	4.3	6.4	10.6	10.6	19.1	74.5

^aAbbreviations: EV, *Eucalyptus*; EC, *Eucalyptus*; R, *Peltogyne* sp.; G, *Gochmatia* sp.; D, *Dipteryx* sp.; A, *Apuleia* sp.; J, *Jacaranda* sp.; P, *Aspidosperma* sp.; and C, *Cedrela* sp.

Table 7. ANN Classification of Charcoal by Source (*Eucalyptus* (E) or Native (N)), Using the Mineral Composition of the Charcoals Produced at Temperatures from 300 °C to 700 °C

observed	Predicted by NIR		correct classification (%)
	E	N	
Training Set			
E	33	1	97.1
N	0	60	100
overall percentage (%)			98.9
Test Set			
E	16	0	100
N	1	30	96.8
overall percentage (%)			97.9

Authors

Geila Santos Carvalho – Departamento de Ciência dos Solos, Universidade Federal de Lavras, 37200-900 Lavras, MG, Brazil
Paulo Ricardo Gerardi Hein – Departamento de Ciências Florestais, Universidade Federal de Lavras, 37200-900 Lavras, MG, Brazil
Alfredo Napoli – Département Persyst, CIRAD UR BioWooEB, F-34398 Montpellier, France
Robert Wojcieszak – Univ. Lille, CNRS, Centrale Lille, ENSCL, Univ. Artois, UMR 8181 - UCCS - Unité de Catalyse et Chimie du Solide, F-59000 Lille, France; orcid.org/0000-0002-8956-5846
Luiz Roberto Guimarães Guilherme – Departamento de Ciência dos Solos, Universidade Federal de Lavras, 37200-900 Lavras, MG, Brazil

Complete contact information is available at:
<https://pubs.acs.org/10.1021/acs.energyfuels.0c01034>

Notes

The authors declare no competing financial interest.

ACKNOWLEDGMENTS

The authors thank the Wood Science and Technology Graduation Program (PPGCTM) and Soil Science Graduation Program (PPGCS) of the Universidade Federal de Lavras (Brazil). Special thanks to CIRAD (Montpellier, France) and UCCS of Université de Lille for analysis and ideas. This study was financed in part by the Coordenação de Aperfeiçoamento de Pessoal de Nível Superior - Brasil (CAPES) – Finance Code 001, by the Conselho Nacional de Desenvolvimento Científico e Tecnológico (CNPq: Grant No. 405085/2016-8)

AUTHOR INFORMATION

Corresponding Author

Fernanda Maria Guedes Ramalho – Departamento de Ciências Florestais, Universidade Federal de Lavras, 37200-900 Lavras, MG, Brazil; orcid.org/0000-0001-5701-4479; Email: fernandaguedesrm@hotmail.com

515 and by Fundação de Amparo à Pesquisa do Estado de Minas
516 Gerais (FAPEMIG). P.R.G.

517 ■ REFERENCES

- 518 (1) Food and Agriculture Organization of the United Nations –
519 FAOSTAT, 2018. < [http://www.fao.org/faostat/en/?fbclid=](http://www.fao.org/faostat/en/?fbclid=IwAR1gUfu0v04mPZDzxUTkxUu092Aq1-Shp1DEpMPtdFAZ3JQXS0aVvlk0N5c#data/FO/visualize)
520 [IwAR1gUfu0v04mPZDzxUTkxUu092Aq1-](http://www.fao.org/faostat/en/?fbclid=IwAR1gUfu0v04mPZDzxUTkxUu092Aq1-Shp1DEpMPtdFAZ3JQXS0aVvlk0N5c#data/FO/visualize)
521 [Shp1DEpMPtdFAZ3JQXS0aVvlk0N5c#data/FO/visualize](http://www.fao.org/faostat/en/?fbclid=IwAR1gUfu0v04mPZDzxUTkxUu092Aq1-Shp1DEpMPtdFAZ3JQXS0aVvlk0N5c#data/FO/visualize)>.
- 522 (2) Indústria Brasileira De Árvores (IBÁ). *Relatório IBÁ 2017*; 2017;
523 80 pp.
- 524 (3) Stange, R.; Vieira, H. C.; Rios, P. D.; Nisgoski, S. Wood and
525 charcoal anatomy of four myrtaceae species. *Cerne* **2018**, *24* (3),
526 190–200.
- 527 (4) BRASIL. 2013. Legislação brasileira sobre meio ambiente.
528 Brasília: Câmara dos Deputados, Edições Câmara, Série e legislação
529 105, Caderno 3 - Temas Internacionais, 186 pp.
- 530 (5) Instituto Brasileiro de Geografia e Estatística (IBGE). *Produção*
531 *da Extração Vegetal e da Silvicultura*, Vol. 31; IBGE: Rio de Janeiro,
532 Brazil, 2016; 54 pp.
- 533 (6) Gonçalves, T. A. P.; Sonsin-Oliveira, J.; Nisgoski, S.; Marcati, C.
534 R.; Ballarin, A. W.; Muñoz, G. I. B. A contribution to the identification
535 of charcoal origin in Brazil III: Microscopic identification of 10
536 Cerrado species. *Aust. J. Bot.* **2018**, *66* (3), 255–264.
- 537 (7) Ramalho, F. M. G.; Hein, P. R. G.; Andrade, J. M.; Napoli, A.
538 Potential of near-infrared spectroscopy for distinguishing charcoal
539 produced from planted and native wood for energy purpose. *Energy*
540 *Fuels* **2017**, *31*, 1593–1599.
- 541 (8) Nisgoski, S.; Magalhães, W. L. E.; Batista, F. R. R.; França, R. F.;
542 Muñoz, G. I. B. de. Anatomical and energy characteristics of charcoal
543 made from five species. *Acta Amazonica* **2014**, *44* (3), 367–372.
- 544 (9) Maruyama, T. M.; Oliveira, L. S.; Britto, A. S., Jr; Nisgoski, S.
545 Automatic classification of native wood charcoal. *Ecological Informatics*
546 **2018**, *46*, 1–7.
- 547 (10) Davrieux, F.; Rousset, P. L. A.; Pastore, T. C. M.; de Macedo,
548 L. A.; Quirino, W. F. Discrimination of native wood charcoal by
549 infrared spectroscopy. *Quim. Nova* **2010**, *33* (5), 1093–1097.
- 550 (11) Costa, L. R.; Trugilho, P. F.; Hein, P. R. G. Evaluation and
551 classification of eucalypt charcoal quality by near infrared spectros-
552 copy. *Biomass Bioenergy* **2018**, *112*, 85–92.
- 553 (12) Weindorf, D. C.; Bakr, N.; Zhu, Y. Advances in portable x-ray
554 fluorescence (pXRF) for environmental, pedological, and agronomic
555 applications. *Adv. Agron.* **2014**, *128*, 1–45.
- 556 (13) Wobraschek, P. Total reflection x-ray fluorescence analysis - a
557 review. *X-Ray Spectrom.* **2007**, *36* (5), 289–300.
- 558 (14) Freitas, D. S.; Rodak, B. W.; Carneiro, M. A. C.; Guilherme, L.
559 R. G. How does Ni fertilization affect a responsive soybean genotype?
560 A dose study. *Plant Soil* **2019**, *441* (1–2), 567–586.
- 561 (15) Pelegrino, M. H. P.; Weindorf, D. C.; Silva, S. H. G.; de
562 Menezes, M. D.; Poggere, G. C.; Guilherme, L. R. G.; Curi, N.
563 Synthesis of proximal sensing, terrain analysis, and parent material
564 information for available micronutrient prediction in tropical soils.
565 *Precision Agriculture* **2019**, *20*, 746–766.
- 566 (16) Penido, E. S.; Martins, G. C.; Mendes, T. B. M.; Melo, L. C. A.;
567 Guimarães, I. R.; Guilherme, L. R. G. Combining biochar and sewage
568 sludge for immobilization of heavy metals in mining soils. *Ecotoxicol.*
569 *Environ. Safety* **2019**, *172*, 326–333.
- 570 (17) Muthukalum, U. A. S. L.; Gunathilake, C. A.; Kalpage, C. S.
571 Removal of heavy metals from industrial wastewater through minerals.
572 *Lecture Notes in Civil Engineering* **2020**, *44*, 615–632.
- 573 (18) Szczepanik, B.; Slomkiewicz, P.; Garnuszek, M.; Czech, K.;
574 Banaš, D.; Kubala-Kukuś, A.; Stabrawa, I. The effect of chemical
575 modification on the physico-chemical characteristics of halloysite:
576 FTIR, XRF, and XRD studies. *J. Mol. Struct.* **2015**, *1084*, 16–22.
- 577 (19) Attaelmanan, A. G.; Mouton, M. Identification of archaeo-
578 logical potsherds excavated at Mleiha using XRF. *Journal of*
579 *Archaeological Science* **2014**, *42* (1), 519–524.
- 580 (20) Kim, K. H.; Kim, T.; Lee, S.; Choi, D.; Yeo, H.; Choi, I.; Choi,
581 J. W. Comparison of physicochemical features of biooils and biochars

- 582 produced from various woody biomasses by fast pyrolysis. *Renewable*
583 *Energy* **2013**, *50*, 188–195.
- (21) Brewer, C. E.; Schmidt-Rohr, K.; Satrio, J. A.; Brown, R. C. 584
Characterization of biochar from fast pyrolysis and gasification 585
systems. *Environ. Progress Sustainable Energy* **2009**, *28* (3), 2009. 586
- (22) Basheer, I. A.; Hajmeer, M. Artificial neural networks: 587
fundamentals, computing, design, and application. *J. Microbiol.* 588
Methods **2000**, *43* (1), 3–31. 589
- (23) Wenshu, L.; Lijun, S.; Jinzhuo, W. Study on wood board defect 590
detection based on artificial neural network. *Open Autom. Control Syst.* 591
J. **2015**, *7*, 290–295. 592
- (24) Castellani, M.; Rowlands, H. Evolutionary artificial neural 593
network design and training for wood veneer classification. *Engineer-* 594
ing Applications of Artificial Intelligence **2009**, *22*, 732–741. 595
- (25) Nisgoski, S.; Oliveira, A. A.; Muñoz, G. I. B. Artificial neural 596
network and SIMCA classification in some wood discrimination based 597
on near-infrared spectra. *Wood Sci. Technol.* **2017**, *51* (4), 929–942. 598
- (26) Cui, X.; Wang, Q.; Zhao, Y.; Qiao, X.; Teng, G. Laser-induced 599
breakdown spectroscopy (LIBS) for classification of wood species 600
integrated with artificial neural network (ANN). *Appl. Phys. B: Lasers* 601
Opt. **2019**, *125* (4), 56. 602
- (27) Yang, Y.; Lin, X.; Wei, B.; Zhao, Y.; Wang, J. Evaluation of 603
adsorption potential of bamboo biochar for metal-complex dye: 604
equilibrium, kinetics and artificial neural network modeling. *Int. J.* 605
Environ. Sci. Technol. **2014**, *11* (4), 1093–1100. 606
- (28) ((28)) Selvanathan, M.; Yann, K. T.; Chung, C. H.; Selvarajoo, 607
A.; Arumugasamy, S. K.; Sethu, V. Adsorption of copper (II) ion from 608
aqueous solution using biochar derived from Rambutan (*Neph-* 609
eliumlappaceum) peel: feedforward neural network modelling study. 610
Water, Air, Soil Pollut. **2017**, *228* (8), 299. 611
- (29) Liao, M.; Kelley, S. S.; Yao, Y. Artificial neural network based 612
modeling for the prediction of yield and surface area of activated 613
carbon from biomass. *Biofuels, Bioprod. Biorefin.* **2019**, *13* (4), 1015– 614
1027. 615
- (30) Cao, H.; Xin, Y.; Yuan, Q. Prediction of biochar yield from 616
cattle manure pyrolysis via least squares support vector machine 617
intelligent approach. *Bioresour. Technol.* **2016**, *202*, 158–164. 618
- (31) Jesus, M. S.; Napoli, A.; Andrade, F. W. C.; Trugilho, P. F.; 619
Rocha, M. F. V.; Gallet, P.; Boutahar, N. Macro ATG Kiln: gaseous 620
flow study in the pyrolysis process of *Eucalyptus* Brazilian. *Journal of* 621
Wood Science **2015**, *6*, 269–274. 622
- (32) Silva, A. L. M.; Cirino, S.; Carvalho, M. L.; Manso, M.; 623
Pessanha, S.; Azeredo, C. D. R.; Carramate, L. F. N. D.; Santos, J. P.; 624
Guerra, M.; Veloso, J. F. C. A. Elemental mapping in a contemporary 625
miniature by full-field X-ray fluorescence imaging with gaseous 626
detector vs. scanning X-ray fluorescence imaging with polycapillary 627
optics. *Spectrochim. Acta, Part B* **2017**, *129*, 1–7. 628
- (33) Bouraoui, Z.; Jeguirim, M.; Guizani, C.; Limousy, L.; Dupont, 629
C.; Gadiou, R. Thermogravimetric study on the influence of 630
structural, textural and chemical properties of biomass chars on 631
CO₂ gasification reactivity. *Energy* **2015**, *88*, 703–710. 632
- (34) Haykin, S. *Redes neurais: princípios e prática*; Bookman: Porto 633
Alegre, Brazil. 2001, 900. 634
- (35) Leite, H. G.; Binoti, D. H. B.; de Oliveira Neto, R. R.; Lopes, P. 635
F.; de Castro, R. R.; Paulino, E. J.; Binoti, M. L. M. S.; Colodette, J. L. 636
Redes neurais artificiais para a estimação da densidade básica da 637
madeira. Artificial neural networks for basic wood density estimation. 638
Sci. Forest. **2016**, *44* (109), 149–154. 639
- (36) Demertzis, K.; Iliadis, L.; Avramidis, S.; El-Kassaby, Y. A. 640
Machine learning use in predicting interior spruce wood density 641
utilizing progeny test information. *Neural Computing and Applications* 642
2017, *28* (3), 505–519. 643
- (37) García-Iruela, A.; Fernández, F. G.; Esteban, L. G.; de Palacios, 644
P.; Simón, C.; Arriaga, F. Comparison of modelling using regression 645
techniques and an artificial neural network for obtaining the static 646
modulus of elasticity of *Pinus radiata* D. Don. timber by ultrasound. 647
Composites, Part B **2016**, *96*, 112–118. DOI: . 648
- (38) Zanuncio, A. J. V.; Carvalho, A. G.; Da Silva, L. F.; Da Silva, M. 649
G.; Carneiro, A. D. C. O.; Colodette, J. L. Prediction of the physical, 650

- mechanical and colorimetric properties of *Eucalyptus grandis* heat-treated wood using artificial neural networks. *Sci. Forest.* **2017**, *45* (113), 109–118.
- (39) Hazir, E.; Koc, K. H. A modeling study to evaluate the quality of wood surface. *Maderas. Ciencia Tecnol.* **2018**, *20* (4), 691–702.
- (40) Chai, H.; Chen, X.; Cai, Y.; Zhao, J. Artificial neural network modeling for predicting wood moisture content in high frequency vacuum drying process. *Forests* **2019**, *10* (1), 16.
- (41) Zanuncio, A. J. V.; Carvalho, A. G.; Silva, L. F. D.; Carneiro, A. D. C. O.; Colodette, J. L. Artificial neural networks as a new tool for assessing and monitoring wood moisture content. *Rev. Arvore* **2016**, *40* (3), 543–549.
- (42) Esteban, L. G.; de Palacios, P.; Conde, M.; Fernández, F. G.; García-Iruela, A.; González-Alonso, M. Application of artificial neural networks as a predictive method to differentiate the wood of *Pinus sylvestris* L. and *Pinus nigra* Arn subsp. *salzmannii* (Dunal) Franco. *Wood Sci. Technol.* **2017**, *51* (5), 1249–1258.
- (43) Nasir, V.; Nourian, S.; Avramidis, S.; Cool, J. Classification of thermally treated wood using machine learning techniques. *Wood Sci. Technol.* **2019**, *53* (1), 275–288.
- (44) Van Nguyen, T. H.; Nguyen, T. T.; Di, J. X.; Do, K. T. L.; Guo, M. Using artificial neural networks (ANN) for modeling predicting hardness change of wood during Heat Treatment. *IOP Conf. Ser.: Mater. Sci. Eng.* **2018**, *394*, No. 032044.